PNAS RESEARCH ARTICLE | IMMUNOLOGY AND INFLAMMATION

NLRP3 is essential for neutrophil polarization and chemotaxis in response to leukotriene B4 gradient

Stijn Van Bruggen[a,b,c], Pierre-André Jarrot[a,b], Eline Thomas[d,e], Casey E. Sheehy[a], Camila M. S. Silva[a,b], Alan Y. Hsu[f,g,h], Pierre Cunin[i], Peter A. Nigrovic[i,j], Edgar R. Gomes[k], Hongbo R. Luo[f,g,h], Clare M. Waterman[c,l], and Denisa D. Wagner[a,b,c,m,1]

Edited by Jenny Ting, The University of North Carolina at Chapel Hill, Chapel Hill, NC; received March 10, 2023; accepted July 21, 2023

Neutrophil recruitment to sites of infection and inflammation is an essential process in the early innate immune response. Upon activation, a subset of neutrophils rapidly assembles the multiprotein complex known as the NLRP3 inflammasome. The NLRP3 inflammasome forms at the microtubule organizing center, which promotes the formation of interleukin (IL)-1β and IL-18, essential cytokines in the immune response. We recently showed that mice deficient in NLRP3 (NLRP3$^{-/-}$) have reduced neutrophil recruitment to the peritoneum in a model of thioglycolate-induced peritonitis. Here, we tested the hypothesis that this diminished recruitment could be, in part, the result of defects in neutrophil chemotaxis. We find that NLRP3$^{-/-}$ neutrophils show loss of cell polarization, as well as reduced directionality and velocity of migration toward increasing concentrations of leukotriene B4 (LTB4) in a chemotaxis assay in vitro, which was confirmed through intravital microscopy of neutrophil migration toward a laser-induced burn injury of the liver. Furthermore, pharmacologically blocking NLRP3 inflammasome assembly with MCC950 in vitro reduced directionality but preserved nondirectional movement, indicating that inflammasome assembly is specifically required for polarization and directional chemotaxis, but not cell motility per se. In support of this, pharmacological breakdown of the microtubule cytoskeleton via nocodazole treatment induced cell polarization and restored nondirectional cell migration in NLRP3-deficient neutrophils in the LTB4 gradient. Therefore, NLRP3 inflammasome assembly is required for establishment of cell polarity to guide the directional chemotactic migration of neutrophils.

neutrophils | NLRP3 inflammasome | cell polarization | chemotaxis

Significance

The importance of the NLRP3 inflammasome in macrophage biology has long been established. However, its role in neutrophil physiology has only recently been described, and remains understudied. The NLRP3 inflammasome is rapidly assembled upon neutrophil activation at the microtubule organizing center (MTOC). Here, we show that NLRP3, in addition to its vital role in inflammasome formation and cytokine secretion, is essential for neutrophil chemotaxis toward an in vitro gradient of leukotriene B4 (LTB4) and to in vivo sterile burn injury, a function unknown for inflammasome until now. Thus, assembly of inflammasome at the MTOC appears to direct cell polarization and directional migration. This observation may have implications for other cell types assembling inflammasome after activation.

The innate immune system is the first line of host defense, which is capable of recognizing and responding to microbial components and endogenous damage molecules, which are called microbial-associated molecular patterns (MAMPs), and damage-associated molecular patterns (DAMPs). These "danger" molecules can trigger downstream inflammatory pathways in order to eliminate pathogens and repair damaged tissue (1). Upon encountering these danger signals, cells of the innate immune system can assemble an intracellular multimeric protein complex called the inflammasome. Inflammasomes are classified based on the sensor protein that oligomerizes in order to form a procaspase-1-activating platform in response to PAMPs and DAMPs (2). Currently, five members of sensor proteins are known to form inflammasomes: the nucleotide-binding oligomerization domain (NOD), leucine-rich repeat (LRR)-containing proteins (NLR) family members (NLRP1, NLRP3, and NLRC4), absent-in-melanoma 2 (AIM2), and pyrin (3, 4). During the assembly process of certain types of inflammasome (NLRP1, NLRP3, and AIM2), a bipartite adaptor protein known as apoptosis-associated speck-like protein containing a caspase-recruitment domain (ASC) facilitates the recruitment of procaspase-1 to the inflammasome complex (5). Procaspase-1 is then activated to form caspase-1 through proximity-induced autocatalysis. Caspase-1 is critical to the inflammatory response by enzymatically cleaving prointerleukin-1β (pro-IL-1β) and pro-IL-18 into their biologically active forms IL-1β and IL-18, respectively, as well as other cellular substrates, such as gasdermin D, to promote lytic cell death, thus magnifying the inflammatory response (6–9).

The NLRP3 inflammasome is among the most studied, and is shown to be of critical importance for host immune defense against bacterial, fungal, and viral infections (10–14). In macrophages, NLRP3 inflammasome formation is a two-step process. Initially, cytoplasmic protein levels of NLRP3 are increased through priming with lipopolysaccharide. Following this priming step, further stimulation of the macrophage will result in oligomerization of NLRP3, ASC and procaspase-1 into the final macromolecular multiprotein structure also termed the ASC speck (15), which assembles at the microtubule organizing center (MTOC) by dynein-directed transport of inflammasome components (16, 17). However,

Author contributions: S.V.B., E.R.G., H.R.L., C.M.W., and D.D.W. designed research; S.V.B., P.-A.J., C.E.S., C.M.S.S., A.Y.H., and P.C. performed research; P.A.N. contributed new reagents/analytic tools; S.V.B., P.-A.J., E.T., and C.S. analyzed data; P.A.N. provided lab equipment; and S.V.B. and D.D.W. wrote the paper.

The authors declare no competing interest.

This article is a PNAS Direct Submission.

[1]To whom correspondence may be addressed. Email: Denisa.wagner@childrens.harvard.edu.

This article contains supporting information online at https://www.pnas.org/lookup/suppl/doi:10.1073/pnas.2303814120/-/DCSupplemental.

Published August 21, 2023.

in addition to macrophages, NLRP3 inflammasome/ASC speck formation has been described as a source of IL-1β production in neutrophils after *Staphylococus aureus* infection or sterile thioglycolate– induced peritonitis (18, 19). As neutrophils are the most abundant leukocyte in circulation and lead the first wave of host defense against both pathogenic infection and tissue damage, this source of IL-1β cannot be overlooked (20). Since this first description of NLRP3 inflammasome formation in neutrophils, ASC speck formation has been described in these cells under both infectious as well as sterile conditions (21–25).

Crucial in the mechanism of inflammation is the proper recruitment and migration of innate immune cells toward the site of injury or infection. Of fundamental importance in this process is adhesion to the endothelium and migration of effector cells through the vessel wall and then toward the source of inflammation, a process which is described as the leukocyte adhesion cascade and chemotaxis (26). This cascade consists of leukocyte rolling, adhesion, and migration. During leukocyte rolling, weak interactions between the leukocyte and endothelial cells, mediated by endothelial selectins with P-selectin glycoprotein ligand 1 (PSGL1) on the leukocyte surface, are formed in close proximity to the site of inflammation (27, 28). The interaction between PSGL1 and E-selectin induces integrin activation (29) to slow and then arrest the rolling by interacting with endothelial ICAM1 and VCAM1 (26). Post arrest, leukocytes translocate through the endothelial barrier, predominantly at endothelial cell–cell junctions (30). Once through the vessel wall, neutrophils are further stimulated by DAMPs and MAMPs (20), which promote their secretion of chemoattractant molecules. One such molecule is the bioactive lipid leukotriene B4 (LTB4), which serves as a secondary chemoattractant molecule, facilitating further neutrophil recruitment (31). LTB4 also serves as a directional cue to guide neutrophil infiltration to the site of insult via directional migration. The sensing of chemotactic gradients by neutrophils is mediated by G-protein-coupled receptors in the plasma membrane, which mediate activation of PI3K signaling in the cell region exposed to the higher concentration of chemoattractant. This promotes establishment of polarized signaling within the neutrophil that results in directional cytoskeletal assembly that drives cell elongation toward the attractant. This polarity is maintained as the cells continue to protrude toward the attractant and retract their rears, thus undergoing directed migration to the site of inflammation (32). The process of tissue infiltration is strictly regulated, as both a reduction or excess in neutrophil recruitment can have devastating consequences for host health, resulting in recurrent infections and chronic inflammation respectively (33–35). In settings of peritonitis, induced through the injection of necrotic cells in the peritoneum, mice deficient in NLRP3 ($NLRP3^{-/-}$) showed a significant reduction in peritoneal neutrophil recruitment (36), similar to the thioglycolate-induced peritonitis (19).

Here, we tested the hypothesis that NLRP3, assembling at the MTOC, directs neutrophil recruitment to sites of inflammation by promoting chemotactic migration. We show that the NLRP3 inflammasome is required for neutrophil polarization and directional movement toward a gradient of leukotriene B4 (LTB4) in vitro. Thus, besides activating surrounding tissues by cytokine release and promoting neutrophil adhesion, NLRP3 has a basic cellular role in establishing cell polarity to mediate directional neutrophil movement.

1. Materials and Methods

1.1. Animals. Both male and female $NLRP3^{-/-}$ (stock n° #021302) and age- and sex-matched wild-type C57BL/6 J ($NLRP3^{+/+}$) (stock n° #000664) mice were obtained from Jackson Laboratory (Bar Harbor, ME, USA). All mouse lines were housed in the animal facilities of the Boston Children's Hospital (Boston, USA) and the Marine Biological Laboratory (Woods Hole, USA). All recurring animal procedures were performed on equivalent timepoints during the day, in order to take circadian rhythms of both laboratory animals and neutrophils into consideration (37). All experimental animal procedures performed in this study were approved by the Institutional Animal Care and Use Committee of Boston Children's Hospital under the protocol numbers 20-01-4096R and 00001378.

1.2. Murine Neutrophils.

1.2.1. Neutrophil isolation. Murine neutrophils were freshly isolated for every experiment from $NLRP3^{-/-}$ and $NLRP3^{+/+}$ mice as previously described (38). In short, on the morning of the experiment, 1 mL of blood was obtained from isoflurane anesthetized mice through the retroorbital plexus into 2 mL of preheated (37 °C) anticoagulant buffer (15 mM EDTA and 1% endotoxin free bovine serum albumin in sterile PBS). The blood was centrifuged at 500 g for 12 min at room temperature, after which the supernatant was discarded, and cells were resuspended in anticoagulant buffer. The resuspended cells were loaded on top of a 3-layer percoll gradient column, containing a 78%/69%/52% percoll in sterile PBS layered in a 15-mL centrifuge tube. After loading the blood cells on top of the 52% layer, the column was centrifuged in a swinging bucket centrifuge for 32 min at 1,500 g at room temperature, with acceleration set at 3, and brake at 0. Cells at the 69%/78% interface were collected, washed, and pelleted by adding sterile PBS and centrifuged for 12 min at 500 g. After red blood cell lysis, through the addition of ammonium-chloride-potassium lysis buffer, cells were resuspended in imaging media (phenol red-free RPMI 1640 supplemented with 10 mM N-2-hydroxyethylpiperazine-N′-2-ethanesulfonic acid) and further used for experimental procedures.

1.2.2. Neutrophil treatment. Isolated neutrophils were either used directly for visualization or pretreated with nocodazole or MCC950 before used in time lapse microscopy. The small molecule inhibitor of inflammasome formation, MCC950 (invivogen), was used to study the effect of inflammasome-free NLRP3. Neutrophils were incubated with 1 μM of MCC950 or vehicle for a period of 30 min at 37 °C and 5% CO_2 prior to chemotaxis assay. For pharmacological disruption of microtubules, neutrophils were incubated with 10 μM of nocodazole (EMD Milipore) or vehicle for 1 h at 37 °C and 5% CO_2. After treatment, neutrophils were washed, pelleted, and resuspended in the appropriate concentration before continuing with time lapse microscopy.

1.3. ASC Speck Visualization/Immunofluorescence. Isolated neutrophils were allowed to adhere to a sterile coverslip for 15 min at 37 °C and 5% CO_2 in a concentration of 6×10^5 cells/mL, after which cells were brought in contact with leukotriene B4 (LTB4) (Merck) for a period of 1 h at 37 °C and 5% CO_2. After LTB4 stimulation, neutrophils were fixed by adding 2% (vol/vol) of paraformaldehyde (PFA) for 30 min at room temperature. After fixation, cells were washed using PBS and permeabilized by adding freshly prepared 0.1% of triton X-100 in PBS for 10 min at 4 °C, after which blocking buffer (2.5% BSA, 0.5% Tween-20 in PBS) was added at 37 °C for 1 h. Cells were incubated at 4 °C overnight with primary antibody directed against ASC (1:800, cell signaling). The next day, cells were washed three times using PBS and incubated with secondary antibody (1:1,500, ThermoFisher) for 2 h at room temperature. After another three washes using PBS, cells were counterstained using Hoechst 33342 (1:10,000, invitrogen) for 10 min at room temperature. After a final wash with PBS, coverslips were mounted and visualized for ASC speck formation. Images were acquired using a Keyence BZ-X810 microscope, equipped with a 60× oil-emersion lens and processed with FIJI/ImageJ (39). ASC speck frequency was determined by capturing 12 Z-stacks of 0.4-μm size from randomized fields of view from the center of the coverslip.

1.4. Transwell Migration and Flow Cytometric Counting. Neutrophils were freshly isolated, after which 10^5 cells were layered on top of a 3-μm porous membrane of a Boyden chamber set-up. Different concentrations of LTB4 were brought in contact with the cells through the bottom chamber. Cells were allowed to migrate to the bottom well for a period of 1 h at 37 °C and 5% CO_2. After migration, the top cell insert was removed and the liquid in the bottom well was collected. Cells were pelleted and resuspended in PBS. After collection, cells were stained for flow cytometric detection of neutrophils through incubation with anti-CD45 and anti-Ly6G antibodies. Neutrophils were identified as CD45-Ly6G double-positive population. Results are depicted as fold increase of migrated cells compared to the unstimulated control sample.

1.5. Time Lapse Visualization by Spinning Disc Confocal and DIC Microscopy. Time-lapse microscopy was performed using isolated peripheral mouse neutrophils from either NLRP3$^{+/+}$ or NLRP3$^{-/-}$ mice. Isolated neutrophils were used directly, or stained using spyDNA (SpiroChrome) or SiR-Tubulin (SpiroChrome) and brought into a μ-chemotaxis slide (IBIDI) at a concentration of 10×10^6/mL. Cells were allowed to adhere for 10 min at 37 °C and 5% CO2 after which a LTB4 gradient was constructed according to the manufacturer's instructions. To study cell movement, the chemotaxis slides were located on a 37 °C prewarmed microscope stage after which three to five random fields per channel were identified. These fields were visualized using a Nikon Eclipse Ti2 microscope equipped with Perfect Focus, a Yokogawa CSU-W spinning disc scanhead, a Nikon motorized stage with xy linear encoders containing a Nano-Z100 piezo insert, and a Hamamatsu Orca-flash 4.0 v3 camera. Confocal and DIC images were acquired every minute for a period of 60 min.

1.6. Laser-Induced Liver Burn Injury and Intravital Microscopy. Induction of liver injury through a laser-induced burn and subsequent intravital microscopy was performed as follows: Mice were anesthetized and injected with Dextran Fluorescein (Thermo Fischer) and PerCP-conjugated anti-Ly6G (Biolegend). Abdominal fur was removed and a midline laparotomy was performed to expose the liver. Next, the imaging apparatus, comprising a suction window attached to a micromanipulator was placed over the exposed liver, and 25 to 35 mmHg of suction (Amvex Corporation) was applied in order to immobilize the liver. Following immobilization, the two-photon Olympus XLUMPLFLN 20× water dipping objective was lowered into place over the suction window. During acquisition, sterile injury was induced by a fixed line of the Chameleon Discovery laser at 1,040 nm. Images were acquired with the tunable line set at 960 nm. 3D imaging was performed using Z stacking with 2-μm Z-stacks, one time point/30 s at a resolution of 512 × 512 for a period of 2.5 h. Neutrophil directionality and migration were analyzed using IMARIS software in a blinded manner. On average, 50 neutrophils per experiment were tracked for the complete 150 min. follow-up period.

1.7. Data Visualization and Statistical Analysis. Rose plots and directionality plots were constructed using Matlab (R2022a – 9.12.0.1975300) using an in-house script (supplement). In the directionality plots, the number of neutrophils at the end of the experiment migrated to one of 16 segments is given as the percentage of the total amount of cells followed. When cells did not migrate more than 10 μm in any direction, they were taken together in the central circle, of which the radius is a measure for the percentage of cells. All data are represented as median ± interquartile range. Statistical analysis was performed using GraphPad Prism (9.3.1). Significance was tested through Mann–Whitney *U* test or unpaired *t* test when comparing two groups, and through a Kruskal–Wallis multiple comparison test for the comparison of more than two groups. $P < 0.05$ was considered statistically significant.

2. Results

2.1. Murine Neutrophils form NLRP3 Inflammasome in Response to LTB4 Stimulation. First, we sought to confirm that in vitro stimulation of primary neutrophils resulted in inflammasome formation in NLRP3$^{+/+}$, but not NLRP3$^{-/-}$ cells (Fig. 1 *A* and *B*). We fixed and immunostained cells for ASC after stimulation with either nigericin or LTB4 for 1 h to assess inflammasome assembly. This showed increased levels of ASC-speck formation in NLRP3$^{+/+}$ neutrophils when stimulated with either nigericin, or 40 and 400 pg/mL of LTB4 compared to NLRP3$^{-/-}$ neutrophils exposed to similar conditions (Fig. 1 *A* and *B*). It should be noted that this single timepoint assay likely underestimates ASC speck formation, which is a dynamic process that is not synchronized among individual cells. However, these results show that, murine neutrophils form NLRP3 inflammasomes in response to LTB4 stimulation (Fig. 1*B*).

2.2. NLRP3 Promotes Rapid Chemotactic Motility in Neutrophils. In order to reach a site of inflammation or infection, neutrophils are required to transmigrate through the endothelial cell layer and migrate through tissue toward chemoattractant molecules released at the site of inflammation. We thus next sought to determine the role of the NLRP3 inflammasome in chemotactic migration. We first examined chemotactic ability using an in vitro transwell chemotaxis assay with LTB4 as chemoattractant. This showed that NLRP3$^{+/+}$ neutrophils chemotaxed significantly better toward LTB4 compared to NLRP3$^{-/-}$ neutrophils (Fig. 2*A*). To determine if the chemotactic defect in NLRP3$^{-/-}$ neutrophils was due to defects in cell migration, we performed time-lapse phase-contrast microscopy of neutrophils migrating in a stable LTB4 gradient established in a microfluidic chamber. Examination of time-lapse videos showed that while a substantial fraction of NLRP3$^{+/+}$ neutrophils migrated rapidly in the direction of higher LTB4 concentration, neutrophils lacking NLRP3 (NLRP3$^{-/-}$) remained largely stationary, independent of their position in the LTB4 gradient (Fig. 2*B*) (Movie S1). Furthermore, single-cell tracking and quantitative analysis of motility parameters showed that NLRP3$^{-/-}$ neutrophils displayed significantly reduced total path length and directional persistence (distance from origin, Fig. 2 *C* and *D*) compared to NLRP3$^{+/+}$ cells. In addition, the mean migration velocity of NLRP3$^{-/-}$ neutrophils was significantly lower compared to NLRP3$^{+/+}$ neutrophils, even in the absence of LTB4 stimulation, although this difference was enhanced by steeper LTB4 gradients (Fig. 2*E*). To determine if NLRP3 contributed to the chemotactic directionality of neutrophil migration, we analyzed motility relative to the direction of the LTB4 gradient. Trajectory plots of cell movement demonstrated that NLRP3$^{+/+}$ neutrophils displayed increasingly biased directional movement toward higher levels of LTB4, while NLRP3$^{-/-}$ neutrophils showed very limited movement with no underlying directionality, independent of the steepness of the LTB4 gradient (Fig. 2*F*). This was further confirmed by Rose plot histograms, (Fig. 2*G*), which showed that neutrophils isolated from NLRP3$^{+/+}$ mice exhibited a marked directional bias toward increasing levels of LTB4, with a very strong bias in movement up a gradient of 4,000 pg/mL of LTB4. In contrast, this directional bias was absent in the neutrophils isolated from NLRP3$^{-/-}$ mice, independent of the LTB4 concentration (Fig. 2*G*). Together, these results show that neutrophils lacking NLRP3 are defective in rapid chemotactic motility toward LTB4, suggesting that NLRP3 is required for chemotactic migration of neutrophils.

2.3. NLRP3 Is Required for Establishing Polarity of the Neutrophil Microtubule Cytoskeleton in Response to an LTB4 Gradient. Chemotactic migration requires translation of the reception of directional chemical cues present in the surrounding environment into spatially constrained subcellular signaling that causes polarization of the microtubule and actin cytoskeletal machinery, resulting in cell protrusion toward the cue to initiate directional motility. Therefore, we sought to determine whether NLRP3 promoted directional chemotactic motility of neutrophils through effects on cell and cytoskeletal polarization. Upon labeling of the neutrophil microtubule cytoskeleton with SiR tubulin and placement of the cells in a stable gradient of LTB4, NLRP3$^{+/+}$ neutrophils lost their rounded shape, became elongated, and started migration toward the increasing concentration of LTB4. In contrast, NLRP3$^{-/-}$ neutrophils remained well spread, relatively circular, and appeared stationary. Quantification of cell area confirmed that loss of NLRP3$^{-/-}$ significantly increased neutrophil spreading as compared to NLRP3$^{+/+}$ neutrophils, even in the absence of stimulation (Fig. 3*A*). To quantify polarization of the neutrophil cytoskeleton, we analyzed the displacement of the MTOC relative to the cell centroid, which would increase with higher polarization (40, 41). In the absence of LTB4

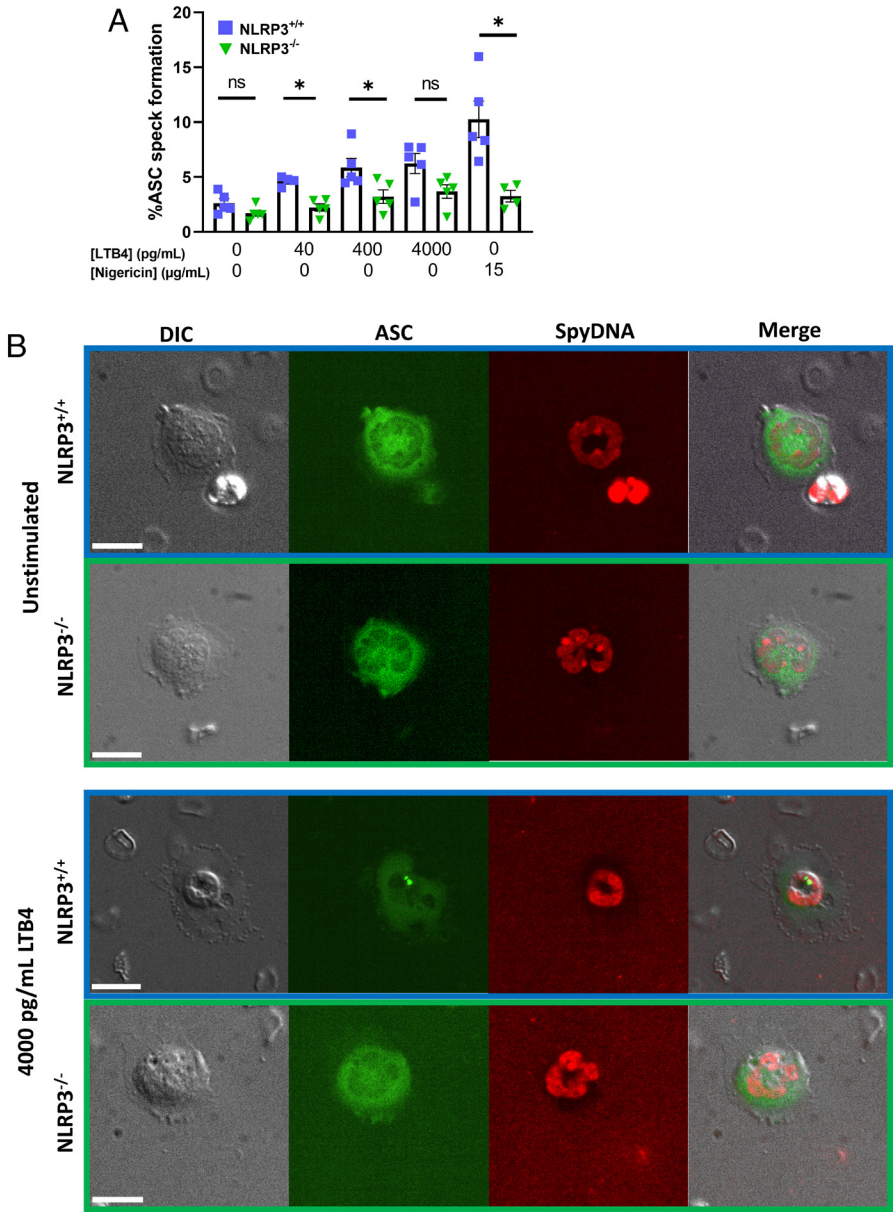

Fig. 1. Stimulation of primary murine neutrophils through leukotriene B4 results in the formation of NLRP3 inflammasome. (*A*) Stimulation of primary isolated murine neutrophils with increasing concentrations of LTB4 resulted in increased occurrence of NLRP3 inflammasome formation, as visualized as ASC-speck in NLRP3$^{+/+}$ neutrophils. In neutrophils deficient in NLRP3 (NLRP3$^{-/-}$), ASC-speck formation was visibly reduced upon LTB4 stimulation. Stimulation of neutrophils through potassium ionophore nigericin was taken as a positive control for inflammasome formation. (*B*) Representative images of isolated neutrophils in absence and presence of LTB4 stimulation (4,000 pg/mL), scale bar represents 10 µm. Mann–Whitney *U* test used for statistical analysis of two groups ($P < 0.05$ *, n = 4 to 5).

stimulation, the MTOC appeared to reside in the cells' center with microtubules emanating from it to the cells' periphery in both NLRP3$^{+/+}$ and NLRP3$^{-/-}$ neutrophils, with microtubules in NLRP3$^{+/+}$ cells notably shorter than those in NLRP3$^{-/-}$ cells (Movie S2). Quantitative analysis of MTOC/centroid displacement confirmed a lack of cytoskeletal polarization in the absence of LTB4 stimulation. However, when NLRP3$^{+/+}$ neutrophils were exposed to a gradient of LTB4, as the cells adopted an elongated morphology, the MTOC and its associated MTs appeared to localize away from the cell center toward one end of the elongated cell, independent of the gradient steepness. In contrast, the LTB4 gradient had no effect on the central position of the MTOC in NLRP3$^{-/-}$ neutrophils (Fig. 3 *B* and *D*). To confirm adoption of a polarized cell shape, we measured cell elongation as the aspect ratio of an ellipse fitted to the cell outline. This showed that when external stimuli were absent, there was no difference in cell elongation between NLRP3$^{+/+}$ and NLRP3$^{-/-}$ neutrophils, with the ratio of the ellipse axes approaching one, representing a circle. However, when stimulated with LTB4, NLRP3$^{+/+}$ but not NLRP3$^{-/-}$ neutrophils showed an increase in elongation (Fig. 3 *C* and *D*). These results show that loss of NLRP3 is associated with a spread morphology as well as an inability of neutrophils to elongate and polarize their MT cytoskeletons relative to an LTB4 gradient, indicating that NLRP3 is required for establishment of neutrophil polarity during chemotaxis.

2.4. NLRP3 Inflammasome Assembly Promotes Directional Movement of Neutrophils. We next sought to determine if NLRP3's requirement in neutrophil chemotaxis was mediated by its function in the inflammasome or by another cytoplasmic activity of NLRP3. To test this, we utilized a small molecule inhibitor, MCC950, which specifically blocks the ability of

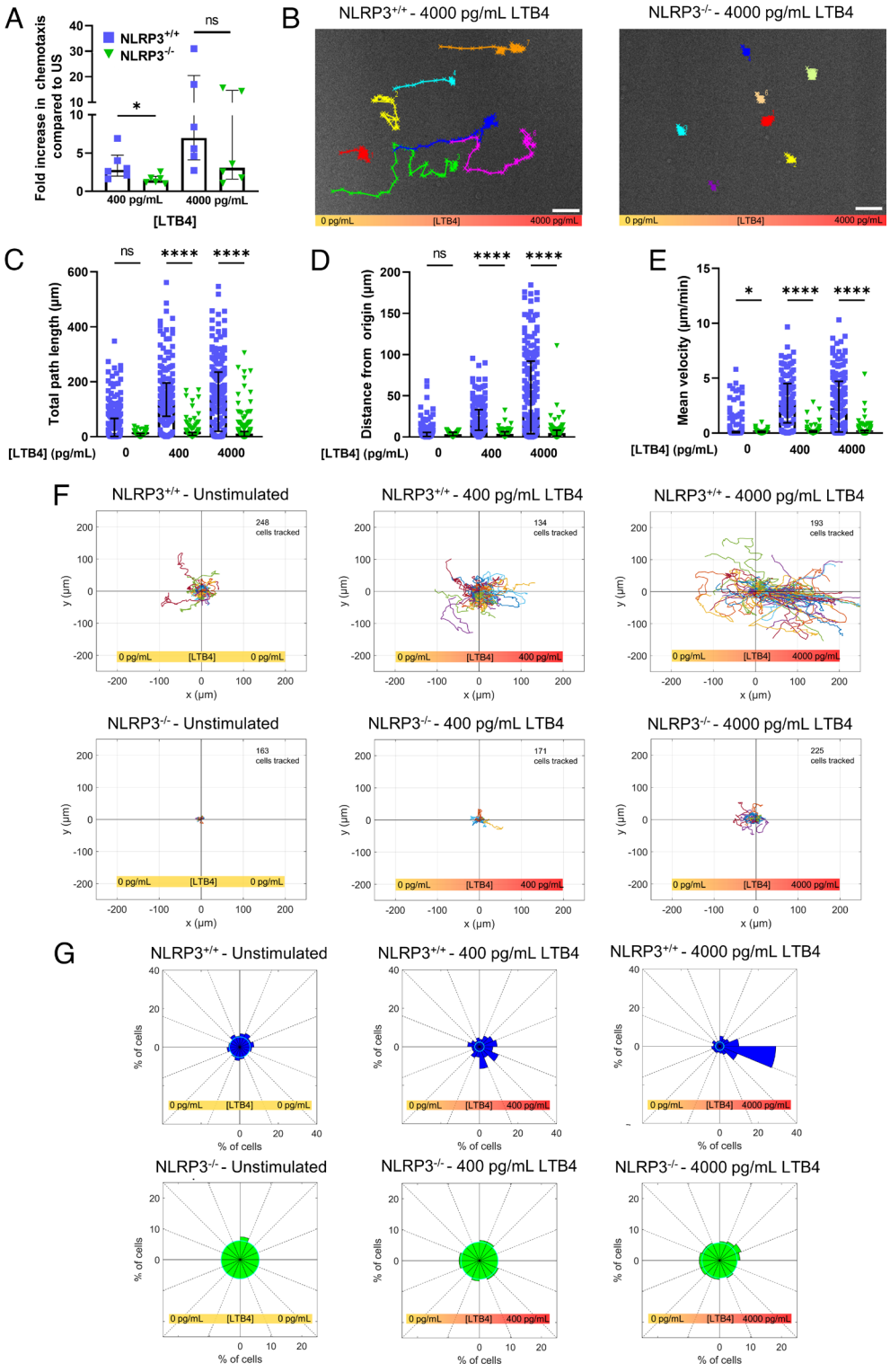

Fig. 2. NLRP3 deficiency impairs proper neutrophil chemotaxis in response to LTB4 gradient. (*A*) Transwell migration of isolated neutrophils through Boyden chamber set-up resulted in reduced migration of NLRP3$^{-/-}$ neutrophils compared to NLRP3$^{+/+}$ cells in the presence of 400 pg/mL LTB4, but not 4,000 pg/mL. (*B*) representative images of NLRP3$^{+/+}$ (*Left*) and NLRP3$^{-/-}$ neutrophils (*Right*) in the presence of a stable 4,000 pg/mL LTB4 gradient. Cells were tracked for a period of 1 h, scale bar represents 50 μm. (*C–E*) Quantification of cellular movement as a result of stimulation using different concentration gradients of LTB4. (*C*) Quantification of total distance traveled of cells in a period of 1 h. (*D*) Distance from the starting point was quantified as the length at which the neutrophil was located at the end of the 1 h follow through live-cell imaging. (*E*) Quantification of the mean velocity at which cells displaced was taken as the average of cellular velocity every minute, taken for a period of 1 h in presence of LTB4 stimulation. (*F*) Rose plots of cellular displacement after 1 h of stimulation using the designated concentration gradients of LTB4. Cellular movement is visualized by bringing the starting point of each cell to the center of the Cartesian coordinate system. Cells were followed for a period of 1 h, the number of cells followed in each condition is depicted in the top right corner of the corresponding rose plot. (*G*) Directionality plots give an unbiased depiction of the direction in which cells traveled upon stimulation through exogenous LTB4. Cells which stayed in the confinement of 10 μm in any direction of the starting point were taken in the central circle of the plot, of which the radius represents the percentage of cells. Percentage of cells which ended up in any of the 16 segments of the directionality plots are represented by the length of the plot in the respective segment. Kruskal–Wallis test was used for statistical analysis of two groups ($P < 0.05$ *, < 0.0001 ****, n = 3 to 6).

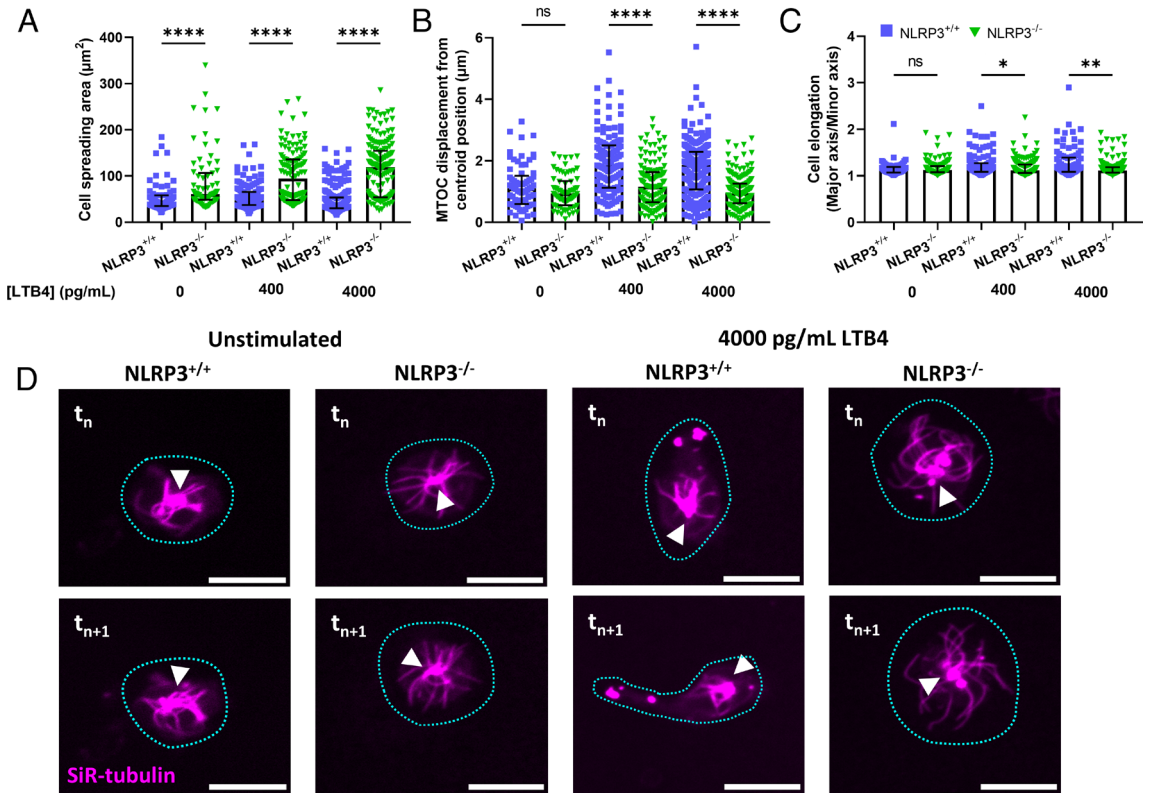

Fig. 3. Deficiency in NLRP3 results in an inability of neutrophils to polarize in response to the presence of an LTB4 gradient. (*A*) Cellular spreading, as quantified by the surface area of the cell in the field of view, is significantly increased in the absence of NLRP3, both in the presence and absence of an LTB4 gradient. (*B* and *C*) quantification of neutrophil polarization through microtubule organizing center displacement (MTOC) and cellular elongation. (*B*) Displacement of the MTOC compared to the cell's centroid position was taken as a measure for cellular polarization. NLRP3$^{-/-}$ neutrophils showed decreased capability for MTOC displacement away from the centroid position upon contact with a extracellular LTB4 gradient. (*C*) Cellular elongation, determined as the ratio of major and minor axis of the best fit ellipse on the cell. Again, a clear decrease in the propensity to elongate was observed in the NLRP3$^{-/-}$ neutrophils. (*D*) representative images of neutrophils, stained through SiR-tubulin, allowing for real-time visualization of the microtubule cytoskeleton. The shape of the cell is indicated through a blue dotted line, and the position of the MTOC is given by white arrowheads. A comparison between neutrophils at timepoint t_n and 1 min later (t_{n+1}) shows a clear polarization of NLRP3$^{+/+}$ but not NLRP3$^{-/-}$ neutrophils, scale bar represents 10 μm. Kruskal–Wallis test was used for statistical analysis of two groups ($P < 0.05$ *, < 0.01 **, < 0.0001 ****, n = 3 to 4).

NLRP3 to assemble into the inflammasome without affecting possible inflammasome-independent functions of NLRP3 (42). Time lapse microscopy and quantitative analysis of neutrophils in a gradient of LTB4 showed that addition of MCC950 to NLRP3$^{+/+}$ neutrophils did not impact general movement, as measured by total path length and mean migration velocity, compared to vehicle alone (Fig. 4 *A* and *C*). However, MCC950 treatment did significantly reduce the directional persistence of NLRP3$^{+/+}$ neutrophil migration, albeit not to the same extent as total loss NLRP3 (Fig. 4*B*). The differential effects of MCC950 on neutrophil motility versus directionality was further confirmed by trajectory and Rose plots, in which NLRP3$^{+/+}$ cells displayed migration paths that were strongly biased in the direction of the LTB4 gradient, while MCC950-treated NLRP3$^{+/+}$ cells had paths with reduced directional bias and NLRP3$^{-/-}$ cells exhibited no directional bias at all (Fig. 4 *D* and *E*). In addition, the effect of MCC950 treatment on cellular elongation and polarization was quantified by measuring the aspect ratio of the best fitted ellipse to the cell outline. Interestingly, the treatment of NLRP3$^{+/+}$ neutrophils in a stable LTB4 gradient with MCC950 resulted in a decrease in the cellular elongation, seen as a decrease in the aspect ratio toward a value of one. Prevention of NLRP3 inflammasome assembly by treatment of neutrophils with MCC950 partially decreased polarity, as the aspect ratio of the ellipse axis of MCC950-treated cells still showed to be elevated as compared to NLRP3$^{-/-}$ cells (Fig. 4*F*). However, confocal imaging of MCC950-treated NLRP3$^{+/+}$ neutrophils in a stable LTB4 gradient showed that they adopted a more circular morphology, resembling NLRP3$^{-/-}$ cells in a similar gradient, while vehicle-treated NLRP3$^{+/+}$ cells showed elongation in the gradient (Fig. 4*G*). These results indicate that the NLRP3 inflammasome is required for formation of an elongated, polarized cell shape in response to an LTB4 gradient, while non-inflammasome functions of NLRP3 may contribute to random cell movement.

2.5. NLRP3 Is Required for the Establishment of Neutrophil Polarization, Thereby Initiating Directional Migration toward an LTB4 Gradient. Chemotaxis requires first the establishment of cell polarization followed by steering of directed motility toward the chemotactic cue. Our data indicate that NLRP3 is required for cell polarization, but it is unclear if NLRP3 is required for steering migration toward LTB4. It is well established that pharmacological disruption of the microtubule cytoskeleton causes neutrophils to adopt an elongated shape in the absence of a chemotactic gradient (43). Therefore, neutrophils were treated with nocodazole (10 μM) to depolymerize the microtubules and induce an elongated state to determine if induction of polarization was sufficient to rescue directional migration of NLRP3$^{-/-}$ cells in an LTB4 gradient. Indeed, we found that nocodazole-treated NLRP3$^{-/-}$ cells showed a cellular elongation response to an LTB4 gradient, which was comparable to both nocodazole-treated NLRP3$^{+/+}$ as well as untreated NLRP3$^{+/+}$ cells (dotted line, controls from Fig. 2), while

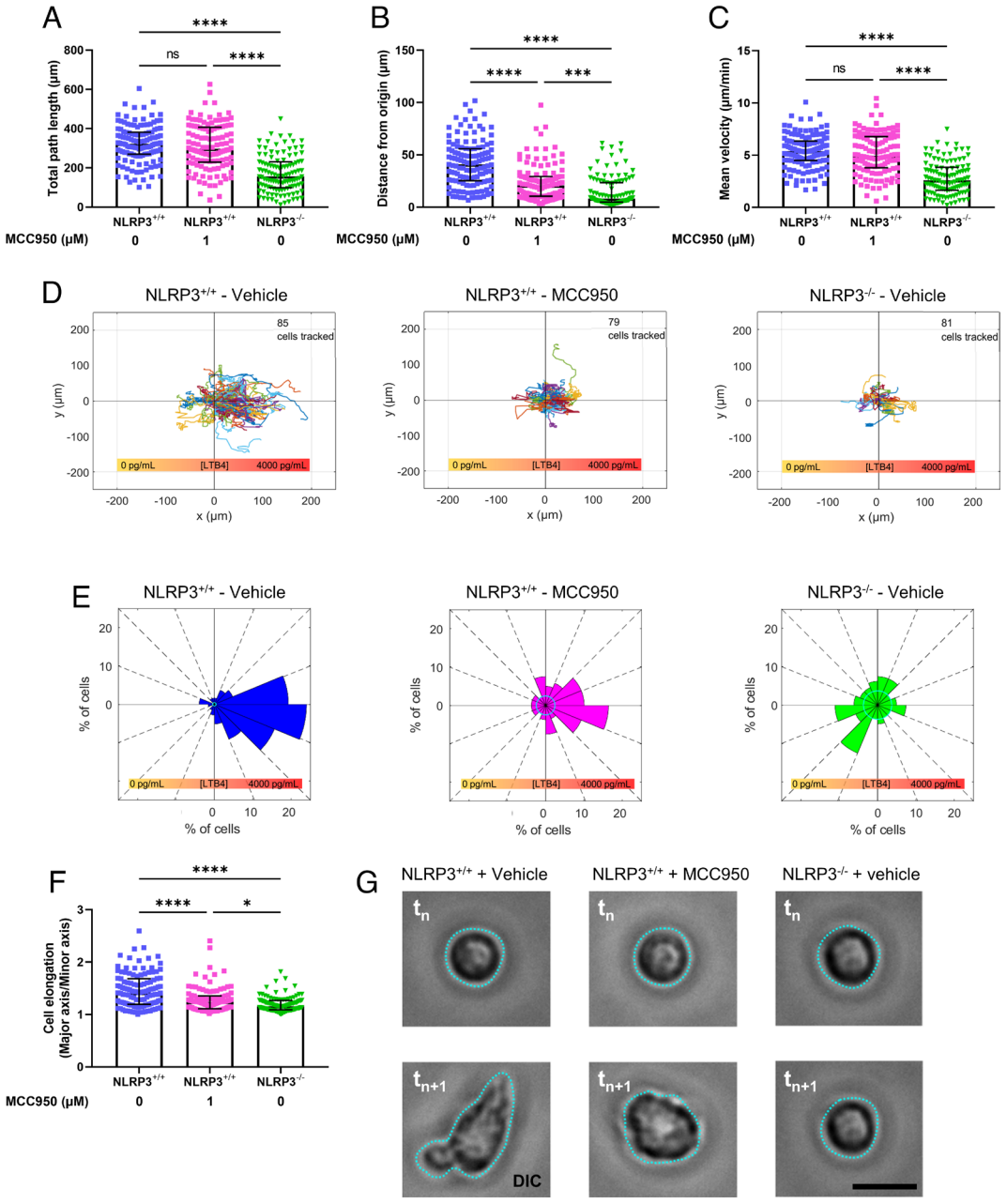

Fig. 4. Inhibition of inflammasome assembly through treatment with MCC950 decreases directional migration of NLRP3$^{+/+}$ neutrophils. (*A*–*C*) Quantification of neutrophil movement in response to a 4,000 pg/mL concentration gradient of LTB4, in the presence or absence of MCC950 pretreatment. (*A*) Quantification of total path length of neutrophils pretreated with either vehicle or MCC950, a small molecule inflammasome assembly inhibitor. (*B*) Distance from origin quantified as the shortest distance to the starting position at the 1-h mark of neutrophil follow-up. Cells were tracked for 1 h following preincubation with MCC950 or vehicle. (*C*) Quantification of mean cellular velocity over a 1-h follow-up period of neutrophils through live-cell imaging. (*D*) Rose plots of neutrophil migration in response to a 4,000 pg/mL LTB4 gradient, with the total number of cells depicted in the top right corner of the corresponding plot. (*E*) Directionality plots of 1-h neutrophil tracking in a stable LTB4 concentration gradient. (*F*) Cellular polarization, quantified through the effect ratio of the best fit ellipse. (*G*) Representative images of cellular elongation in response to LTB4 gradient. Images were taken randomly during the 1-h follow-up (t_n) and 1 min late (t_{n+1}) to show the dynamic motion of cells in response to external LTB4 gradient of 4,000 pg/mL. MCC950 drastically reduced distance traveled from the origin and the extent of NLRP3$^{+/+}$ neutrophil elongation. Kruskal–Wallis test was used for statistical analysis of two groups ($P < 0.001$ ***, < 0.0001 ****, n = 4).

vehicle-treated NLRP3$^{-/-}$ cells did not show an elongation response (Fig. 5 *A* and *B*). Examination of motility parameters showed that nocodazole treatment of NLRP3$^{-/-}$ neutrophils significantly increased the total path length, directional persistence, and velocity as compared to vehicle-treated NLRP3$^{-/-}$ neutrophils, indicating that induction of cell polarity was sufficient to rescue the defects in migration caused by loss of NLRP3. However, nocodazole-treated NLRP3$^{-/-}$ neutrophils still showed a significant decrease in total migration, directionality of migration, and velocity compared to nocodazole-treated NLRP3$^{+/+}$ cells and vehicle-treated NLRP3$^{+/+}$ cells (dotted line, controls from Fig. 2) (Fig. 5 *C*–*E*). Importantly, rose plots showed that nocodazole-induced motility of NLRP3$^{-/-}$ cells lacked a sense of direction and was randomly oriented with respect to the LTB4 gradient (Fig. 5 *F* and *G*). Together with our other findings, we conclude that the NLRP3 inflammasome promotes directional chemotaxis to an LTB4 gradient through initiation of a polarized state that is required for directional neutrophil movement.

2.6. Absence of NLRP3 Prevents In Vivo Neutrophil Swarming toward a Laser-Induced Liver Burn Injury. To visualize individual neutrophil movement in vivo, we adopted the laser-induced

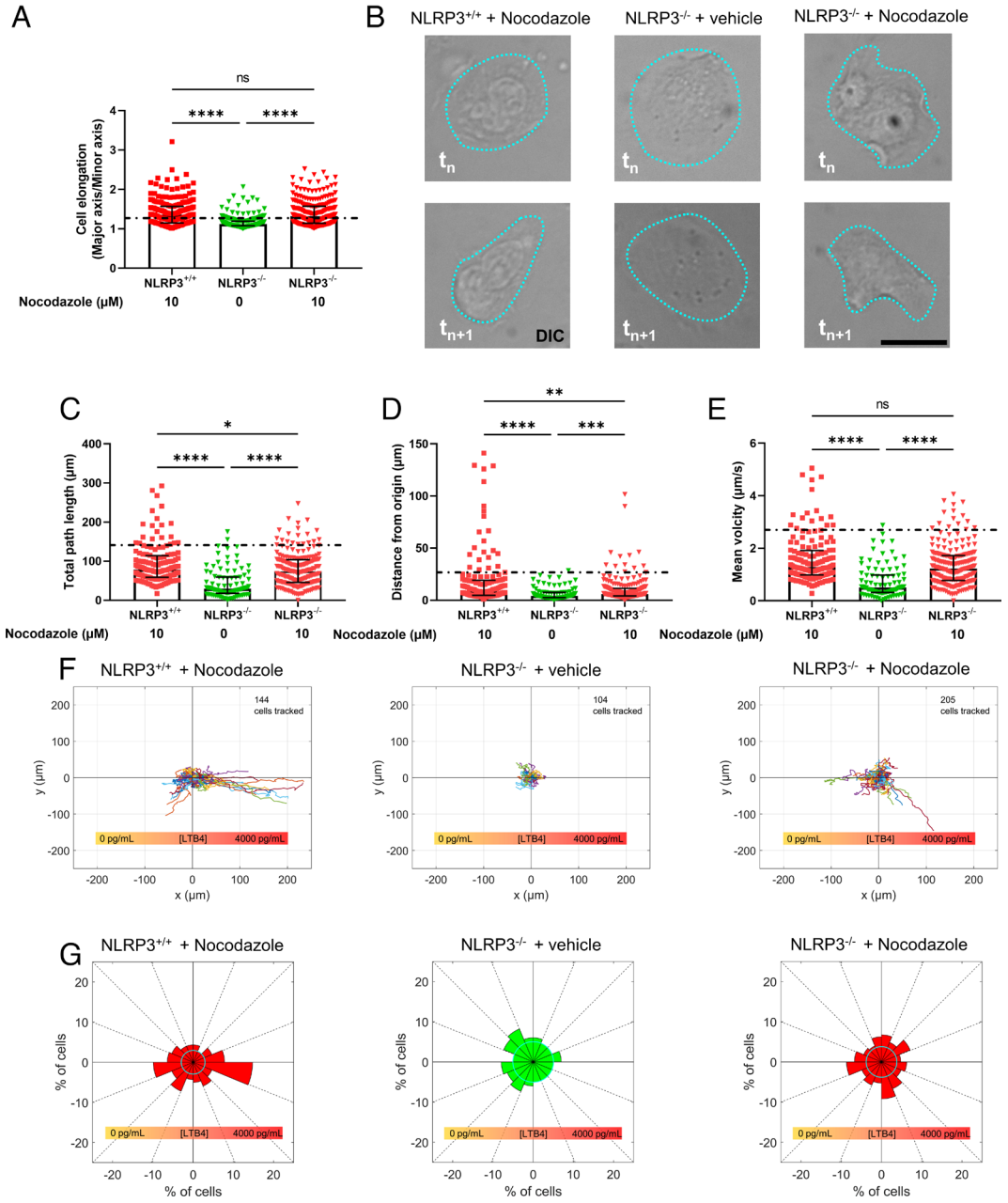

Fig. 5. Pharmacological break-down of the microtubule cytoskeleton by nocodazole rescues cellular movement but not directionality of NLRP3-deficient neutrophils. (*A*) Vehicle-treated NLRP3$^{-/-}$ neutrophils showed a clear impairment of cellular elongation, quantified through the effect ratio of the best fit ellipse. (*B*) Representative images of cellular elongation in response to LTB4 gradient. Images were taken randomly during the 1-h follow-up (t_n) and 1 min late (t_{n+1}) to show the dynamic motion of cells in response to external LTB4 gradient of 4,000 pg/mL. While nocodazole promoted NLRP3$^{-/-}$ cell elongation and migration, it did not improve chemotaxis toward the LTB4 gradient. (*C–E*) Quantification of cellular movement of neutrophils following real-time tracking of cells in the presence of a 4,000 pg/mL gradient of LTB4. Prior to exposure to LTB4 gradients, neutrophils were pretreated for 1 h with nocodazole or vehicle in order to break down the microtubule cytoskeleton. The mean of NLRP$^{+/+}$ neutrophils, taken from (Fig. 2 *C* and *D*) are depicted as a dotted line. Total distance traveled of neutrophils over a 1-h time period in an LTB4 gradient. Treatment of NLRP3$^{-/-}$ neutrophils with nocodazole increased their migration significantly as compared to vehicle-treated NLRP3$^{-/-}$ neutrophils. (*F*) Rose plots of cellular movement confirm that NLRP3$^{-/-}$ neutrophils show increased movement as compared to vehicle-treated NLRP3$^{-/-}$ cells. However, cellular migration of NLRP3$^{+/+}$ cells, treated with nocodazole, was still significantly higher. (*G*) Directionality plots show that the treatment of NLRP3$^{-/-}$ neutrophils with nocodazole resulted in a migration without a bias as regard to direction, directionality was also reduced in NLRP3$^{+/+}$ neutrophils treated with nocodazole. Kruskal–Wallis test was used for statistical analysis of two groups ($P < 0.05$ *, < 0.01 **, < 0.001 ***, < 0.0001 ****, n = 6).

liver injury intravital microscopy model (44). Neutrophils were rapidly recruited toward the site of the injury in NLRP3$^{+/+}$ mice. However, this chemotactic migration was significantly reduced in NLRP3$^{-/-}$ mice (Movie S3). Starting 30 min. after induction of the sterile injury a clear increase in the directional migration of neutrophils toward the site of the burn injury was observed only in the NLRP3$^{+/+}$ mice. For the remaining 120 min. of the observation period, similar yet less pronounced observations were made (Fig. 6*A*). When quantifying neutrophil directionality and migratory pathways for the whole experimental period, the directionality of migration toward the site of injury is clearly visible for NLRP3$^{+/+}$, seen as directionality arrows pointing mostly toward the site of laser-induced burn injury in the NLRP3$^{+/+}$ mice (Fig. 6*B*). For NLRP3$^{-/-}$ mice, this directionality is greatly affected, seen by a reduction in arrow length, as well as more unspecific migration (Fig. 6*B*). This was confirmed by determining

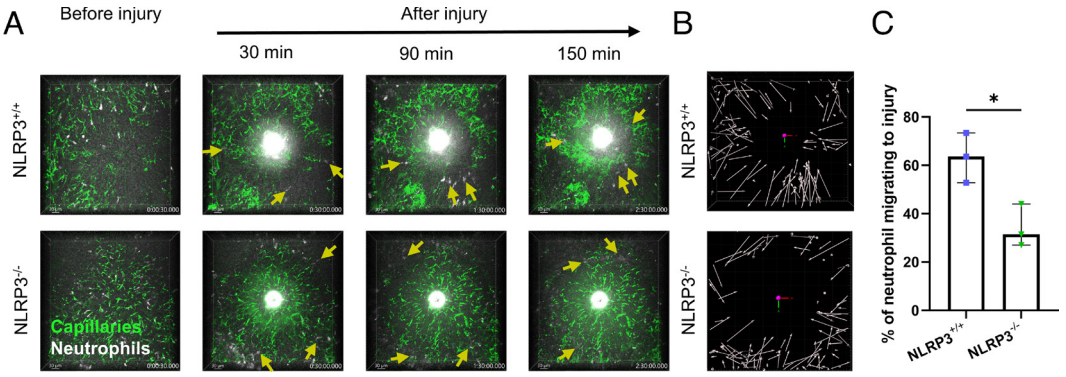

Fig. 6. NLRP3 deficiency reduces neutrophil chemotaxis toward a laser-induced liver burn injury. (*A*) Representative intravital microscopy images acquired every 30 s for a period of 150 min following laser-induced liver burn injury. Neutrophil migration toward the burn was tracked during this period. Neutrophils are highlighted by yellow arrows, directionality of the arrow depicts the direction of neutrophil migration in the next frame. We observed an increase in blood vessel dextran leakage in the livers of NLRP3$^{+/+}$ mice following injury, seen as an increasing area of green fluorescence outside the liver microvasculature. (*B*) Visualization of neutrophil tracking during the 150-min follow-up period. Arrows depict the start and end point of the neutrophil during the 150 min of follow-up. (*C*) Quantification of the fraction of neutrophils that migrated toward the site of injury over the 150-min follow-up period by a blinded investigator, presented as the percentage of neutrophils from the total number of neutrophils inside the field of view during the follow-up period. Unpaired *t* test was used for statistical analysis of two groups ($P < 0.05$ *, n = 3).

the percentage of neutrophils migrating toward the site of the burn injury by a blinded investigator. Quantification of this process of directed neutrophil migration revealed a significant increase in the percentage of neutrophils migrating toward the burn injury in NLRP3$^{+/+}$ mice compared to NLRP3$^{-/-}$ mice (Fig. 6*C*). These in vivo observations further support the role of NLRP3 in neutrophil chemotaxis.

3. Discussion

In this study, we provide evidence for an intracellular function of neutrophil inflammasome. We have recently observed that neutrophil-derived, NLRP3-dependent IL-1β released early in inflammation increases venular cell adhesion molecule expression, which favors neutrophil extravasation. We further identified that NLRP3 is required for neutrophil recruitment to the peritoneum in a model of thioglycolate-induced peritonitis (19). We now show here that formation of the NLRP3 inflammasome at the neutrophil MTOC (25) is necessary for neutrophil polarization, required for directional migration toward an in vitro gradient of the important chemoattractant LTB4.

Beside chemotaxis, LTB4 is known to activate neutrophils toward the formation of neutrophil extracellular traps (NETs) (45). Essential in NETosis is the activation of the NLRP3 inflammasome (24). Indeed, upon stimulation of NLRP3$^{+/+,}$ but not NLRP3$^{-/-}$ neutrophils with LTB4, we observed an ASC-speck in a subset of cells. ASC speck forms very early in the activation process indicating that it may have many cellular functions before inducing death by pyroptosis/NETosis in some cells. Guided by the observation that NLRP3-deficient neutrophils show reduced extravasation into the peritoneum upon injection of the chemical irritant thioglycolate (19), we decided to study neutrophil chemotaxis in vitro. Indeed, NLRP3$^{-/-}$ neutrophils showed decreased chemotactic potential in a Boyden chamber set-up, using LTB4 as a chemoattractant. These findings were further supported by a reduction in cellular migration toward a gradient of LTB4 in real time, visualized through time-lapse imaging of NLRP3$^{-/-}$ neutrophils. In addition to showing a marked reduction in overall movement, the directionality of movement of NLRP3$^{-/-}$ cells was significantly decreased, and resembled random migration rather than directional chemotaxis toward higher concentrations of LTB4.

Prior to cellular migration and chemotaxis, neutrophil polarization plays a key role in sensing chemotactic molecules. Of special importance is the cellular location of the MTOC, and its radiating microtubules, as these structures are in part responsible for vesicular transport, thereby creating a polarized asymmetry inside the cell (46, 47). In contrast to NLRP3-positive cells, in NLRP3$^{-/-}$ neutrophils, MTOC displacement from the cell center as part of polarization of the cells was minimal in response to a gradient of LTB4. These results imply a direct role for the NLRP3 inflammasome in the formation of a polarized cell morphology, essential for neutrophil chemotaxis. Until now, a direct link between the NLRP3 inflammasome and the basic cell biology of motility or directional migration was not described. The inflammasome is known to be a vital regulator of inflammation through maturation of inflammatory cytokines (48). However, the release of these inflammatory cytokines needs to be perfectly timed and strictly regulated to take place at the correct time, and location. Therefore, the close interaction between cytokine production and chemotaxis may be of importance.

A distinction has to be made between the role of cytoplasmic NLRP3, and NLRP3 associated with the inflammasome. The small molecule inhibitor of inflammasome assembly and activation, MCC950, has been shown to attenuate disease symptoms and progression in several inflammatory disease models e.g., experimental autoimmune encephalomyelitis (42), spontaneous colitis (49), and myocardial infarction (50, 51). In order to assess the importance of inflammasome assembly in chemotaxis, we treated neutrophils with MCC950 prior to cellular tracking in response to LTB4. Interestingly, MCC950 treatment of NLRP3$^{+/+}$ neutrophils did not have a marked effect on the distance of neutrophil migration, but negatively affected directionality of movement. This reduction in directionality of MCC950-treated NLRP3$^{+/+}$ neutrophils can be explained by the observed inhibition of the elongation/polarization of the neutrophils in response to the LTB4 gradient, as the treatment with MCC950 rendered NLRP3$^{+/+}$ neutrophils more rounded, and comparable to the morphology of NLRP3$^{-/-}$ neutrophils, while vehicle-treated NLRP3$^{+/+}$ cells took on an elongated morphology in similar gradients of LTB4. Therefore, it is the assembly of the NLRP3 protein in the NLRP3 inflammasome complex which is required for neutrophil polarization prior to chemotaxis. However, MCC950 treatment only resulted in a

partial inhibition of movement of NLRP3$^{+/+}$ neutrophils, something which can possibly be explained by an incomplete inhibition of the NLRP3 inflammasome formation by the drug under our experimental conditions or by a yet unknown alternative function of soluble NLRP3 molecules in motility.

Neutrophil chemotaxis requires a spatiotemporal regulation of intracellular signaling events. These intracellular signaling events affect both microtubules and actin cytoskeleton, both of which are essential for neutrophil polarization (43, 52). Central in this signaling cascade is the activation of Rho, a family of small GTPases, which control the dynamic organization of the actin cytoskeleton, thereby providing the required forces for cell motility (53). Sequestration of these Rho GTPases by the microtubules is known to inhibit their activity, thereby suppressing neutrophil polarization. Disruption of the microtubule cytoskeleton, e.g., by nocodazole treatment, causes Rho activation, polarization, and cellular migration of wild-type neutrophils (43, 54). In NLRP3$^{-/-}$ neutrophils, pretreatment with nocodazole resulted in a partial rescue of the migratory phenotype when compared to NLRP3$^{+/+}$ neutrophils treated with similar concentrations of nocodazole. However, nocodazole treatment of NLRP3$^{+/+}$ cells impaired directional migration, a finding which is in line with previous studies performed in dHL-60 cells (43). Nevertheless, microtubule disruption through nocodazole treatment resulted in a significant increase in overall movement of NLRP3$^{-/-}$ cells as compared to vehicle-treated NLRP3$^{-/-}$ neutrophils. In addition, nocodazole treatment of the NLRP3$^{-/-}$ cells resulted in a complete rescue of LTB4-induced elongation of the cells. Despite the artificial rescue of neutrophil polarization by nocodazole, the NLRP3$^{-/-}$ cells were unable to migrate toward the chemotactic gradient.

Finally, we wished to visualize neutrophil chemotaxis to tissue injury through intravital microscopy to confirm NLRP3 importance in an in vivo model. We chose a sterile liver injury induced by a laser to evaluate the physiological role of NLRP3, in neutrophil migration toward the wound. We observed a clear defect in the directionality of movement of neutrophils toward the wound in the NLRP3$^{-/-}$ livers, in accordance with our in vitro observations.

4. Conclusion

The role of the NLRP3 inflammasome in neutrophils has long been overlooked. However, in recent years, its implications in neutrophil activation and function have been established in several pathogen-induced, as well as sterile settings of inflammation. Here, the role of NLRP3, and its assembly in the NLRP3 inflammasome, is shown to play an essential role in neutrophil polarization to mediate directional migration and chemotaxis in vitro toward a gradient of LTB4. In addition, in vivo migration toward a sterile liver burn injury was observed to be reduced in the absence of NLRP3 as well. These findings in combination with recently published work from our group broadens the knowledge of neutrophil NLRP3 inflammasome and serves as the stepping stone for further investigation into the mechanistic role of the NLRP3 inflammasome in the signaling cascade resulting in neutrophil activation and chemotaxis. In addition, this work reveals questions about inflammasomes in other polarized or migratory cells.

Data, Materials, and Software Availability. Microscopy files – Live cell imaging files (analyzed data) data have been deposited in Figshare (https://doi.org/10.6084/m9.figshare.23816418; https://figshare.com/articles/dataset/CombinedData_VanBruggenEtal_xlsx/23816418). Some study data available (Raw life cell imaging data files are too big, but we hereby confirm that upon reasonable request, the raw data for the publication will be shared).

ACKNOWLEDGMENTS. In addition, we would like to thank the Marine Biological Laboratory (MBL) for support as Denisa Wagner and Clare Waterman are part of the Whitman Center faculty. We would like to thank Nikon Instruments, with a special thanks to Stephen Ross, for the loan and help with the microscopy equipment at MBL. S.V.B. would like to thank the Belgian American Educational Foundation and the Fonds Wetenschappelijk Onderzoek Vlaanderen for granting the funding, allowing this collaboration. A.Y.H. received T32 funding the NRSA institutional Postdocotoral training grant (n° 5T32HL066987-20). P.C. was supported by the grant K01AR078975. P.A.N. is funded by R01AR065538 and P30AR070253. C.M.W. is supported by the Division of Intramual Research at the National Heart, Lung, and Blood Institute at the NIH. D.D.W. is funded by a grant from the NIH (R35 HL135765) and by a kind gift from the Berzin family.

Author affiliations: [a]Program in Cellular and Molecular Medicine, Boston Children's Hospital, Boston, MA 02115; [b]Department of Pediatrics, Harvard Medical School, Boston, MA 02115; [c]Whitman Center, Marine Biological Laboratory, Chicago University, Woods Hole, MA 02543; [d]Department of Life Science Technology, Imec, Leuven 3001, Belgium; [e]Department of Biophysics, Katholieke Universiteit Leuven, Leuven 3000, Belgium; [f]Department of Pathology, Harvard Medical School, Boston, MA 02115; [g]Department of Pathology, Dana-Farber/Harvard Cancer Center, Boston, MA 02115; [h]Department of Laboratory Medicine, Boston Children's Hospital, Boston, MA 02115; [i]Division of Immunology, Department of Pediatrics, Boston Children's Hospital, Harvard Medical School, Boston, MA 02115; [j]Division of Rheumatology, Inflammation, and Immunity, Department of Medicine, Brigham and Women's Hospital, Boston, MA 02115; [k]Instituto de Medicina Molecular João Lobo Antunes, Faculdade de Medicina da Universidade de Lisboa, Lisbon 1649-028, Portugal; [l]Cell Biology and Physiology Center, National Heart, Lung, and Blood Institute of the NIH, Bethesda, MD 20892; and [m]Division of Hematology/Oncology, Boston Children's Hospital, Boston, MA 02115

1. O. Takeuchi, S. Akira, Pattern recognition receptors and inflammation. *Cell* **140**, 805–820 (2010).
2. L. Franchi, T. Eigenbrod, R. Munoz-Planillo, G. Nunez, The inflammasome: A caspase-1-activation platform that regulates immune responses and disease pathogenesis. *Nat. Immunol.* **10**, 241–247 (2009).
3. D. Sharma, T. D. Kanneganti, The cell biology of inflammasomes: Mechanisms of inflammasome activation and regulation. *J. Cell Biol.* **213**, 617–629 (2016).
4. M. Lamkanfi, V. M. Dixit, Mechanisms and functions of inflammasomes. *Cell* **157**, 1013–1022 (2014).
5. T. Fernandes-Alnemri *et al.*, The pyroptosome: A supramolecular assembly of ASC dimers mediating inflammatory cell death via caspase-1 activation. *Cell Death Differ* **14**, 1590–1604 (2007).
6. L. Franchi, N. Warner, K. Viani, G. Nunez, Function of Nod-like receptors in microbial recognition and host defense. *Immunol. Rev.* **227**, 106–128 (2009).
7. F. Martinon, K. Burns, J. Tschopp, The inflammasome: A molecular platform triggering activation of inflammatory caspases and processing of proIL-beta. *Mol. Cell* **10**, 417–426 (2002).
8. G. A. Manji *et al.*, PYPAF1, a PYRIN-containing Apaf1-like protein that assembles with ASC and regulates activation of NF-kappa B. *J. Biol. Chem.* **277**, 11570–11575 (2002).
9. J. Shi *et al.*, Cleavage of GSDMD by inflammatory caspases determines pyroptotic cell death. *Nature* **526**, 660–665 (2015).
10. T. D. Kanneganti *et al.*, Critical role for Cryopyrin/Nalp3 in activation of caspase-1 in response to viral infection and double-stranded RNA. *J. Biol. Chem.* **281**, 36560–36568 (2006).
11. K. Schroder, J. Tschopp, The inflammasomes. *Cell* **140**, 821–832 (2010).
12. P. G. Thomas *et al.*, The intracellular sensor NLRP3 mediates key innate and healing responses to influenza A virus via the regulation of caspase-1. *Immunity* **30**, 566–575 (2009).
13. A. Grebe, F. Hoss, E. Latz, NLRP3 Inflammasome and the IL-1 Pathway in Atherosclerosis. *Circ. Res.* **122**, 1722–1740 (2018).
14. O. Gross *et al.*, Syk kinase signalling couples to the Nlrp3 inflammasome for anti-fungal host defence. *Nature* **459**, 433–436 (2009).
15. B. S. Franklin, E. Latz, F. I. Schmidt, The intra- and extracellular functions of ASC specks. *Immunol. Rev.* **281**, 74–87 (2018).
16. V. G. Magupalli *et al.*, HDAC6 mediates an aggresome-like mechanism for NLRP3 and pyrin inflammasome activation. *Science* **369** (2020).
17. A. Pandey, C. Shen, S. Feng, S. M. Man, Cell biology of inflammasome activation. *Trends Cell Biol.* **31**, 924–939 (2021).
18. J. S. Cho *et al.*, Neutrophil-derived IL-1beta is sufficient for abscess formation in immunity against *Staphylococcus aureus* in mice. *PLoS Pathog.* **8**, e1003047 (2012).
19. S. Fukui *et al.*, NLRP3 inflammasome activation in neutrophils directs early inflammatory response in murine peritonitis. *Sci. Rep.* **12**, 21313 (2022).
20. S. de Oliveira, E. E. Rosowski, A. Huttenlocher, Neutrophil migration in infection and wound repair: Going forward in reverse. *Nat. Rev. Immunol.* **16**, 378–391 (2016).
21. T. C. Tzeng *et al.*, A fluorescent reporter mouse for inflammasome assembly demonstrates an important role for cell-bound and free ASC specks during in vivo infection. *Cell Rep.* **16**, 571–582 (2016).
22. K. W. Chen *et al.*, The neutrophil NLRC4 inflammasome selectively promotes IL-1beta maturation without pyroptosis during acute Salmonella challenge. *Cell Rep.* **8**, 570–582 (2014).
23. M. Karmakar, M. A. Katsnelson, G. R. Dubyak, E. Pearlman, Neutrophil P2X7 receptors mediate NLRP3 inflammasome-dependent IL-1beta secretion in response to ATP. *Nat. Commun.* **7**, 10555 (2016).
24. P. Munzer *et al.*, NLRP3 inflammasome assembly in neutrophils is supported by PAD4 and promotes NETosis under sterile conditions. *Front Immunol.* **12**, 683803 (2021).

25. K. Aymonnier *et al.*, Inflammasome activation in neutrophils of patients with severe COVID-19. *Blood Adv.* **6**, 2001–2013 (2022).
26. S. Nourshargh, R. Alon, Leukocyte migration into inflamed tissues. *Immunity* **41**, 694–707 (2014).
27. G. S. Kansas, Selectins and their ligands: Current concepts and controversies. *Blood* **88**, 3259–3287 (1996).
28. R. P. McEver, R. D. Cummings, Role of PSGL-1 binding to selectins in leukocyte recruitment. *J. Clin. Invest.* **100**, S97–103 (1997).
29. S. I. Simon, Y. Hu, D. Vestweber, C. W. Smith, Neutrophil tethering on E-selectin activates beta 2 integrin binding to ICAM-1 through a mitogen-activated protein kinase signal transduction pathway. *J. Immunol.* **164**, 4348–4358 (2000).
30. M. Phillipson *et al.*, Vav1 is essential for mechanotactic crawling and migration of neutrophils out of the inflamed microvasculature. *J. Immunol.* **182**, 6870–6878 (2009).
31. P. V. Afonso *et al.*, LTB4 is a signal-relay molecule during neutrophil chemotaxis. *Dev. Cell* **22**, 1079–1091 (2012).
32. L. Gambardella, S. Vermeren, Molecular players in neutrophil chemotaxis–focus on PI3K and small GTPases. *J. Leukoc. Biol.* **94**, 603–612 (2013).
33. E. Kolaczkowska, P. Kubes, Neutrophil recruitment and function in health and inflammation. *Nat. Rev. Immunol.* **13**, 159–175 (2013).
34. S. Caielli, J. Banchereau, V. Pascual, Neutrophils come of age in chronic inflammation. *Curr. Opin. Immunol.* **24**, 671–677 (2012).
35. N. Borregaard, Neutrophils, from marrow to microbes. *Immunity* **33**, 657–670 (2010).
36. S. S. Iyer *et al.*, Necrotic cells trigger a sterile inflammatory response through the Nlrp3 inflammasome. *Proc. Natl. Acad. Sci. U.S.A.* **106**, 20388–20393 (2009).
37. A. Aroca-Crevillen, J. M. Adrover, A. Hidalgo, Circadian features of neutrophil biology. *Front Immunol.* **11**, 576 (2020).
38. M. Demers *et al.*, Cancers predispose neutrophils to release extracellular DNA traps that contribute to cancer-associated thrombosis. *Proc. Natl. Acad. Sci. U.S.A.* **109**, 13076–13081 (2012).
39. J. Schindelin *et al.*, Fiji: An open-source platform for biological-image analysis. *Nat. Methods* **9**, 676–682 (2012).
40. A. I. Gotlieb, L. M. May, L. Subrahmanyan, V. I. Kalnins, Distribution of microtubule organizing centers in migrating sheets of endothelial cells. *J. Cell Biol.* **91**, 589–594 (1981).
41. A. Kupfer, D. Louvard, S. J. Singer, Polarization of the Golgi apparatus and the microtubule-organizing center in cultured fibroblasts at the edge of an experimental wound. *Proc. Natl. Acad. Sci. U.S.A.* **79**, 2603–2607 (1982).
42. R. C. Coll *et al.*, A small-molecule inhibitor of the NLRP3 inflammasome for the treatment of inflammatory diseases. *Nat. Med.* **21**, 248–255 (2015).
43. J. Xu, F. Wang, A. Van Keymeulen, M. Rentel, H. R. Bourne, Neutrophil microtubules suppress polarity and enhance directional migration. *Proc. Natl. Acad. Sci. U.S.A.* **102**, 6884–6889 (2005).
44. B. McDonald *et al.*, Intravascular danger signals guide neutrophils to sites of sterile inflammation. *Science* **330**, 362–366 (2010).
45. M. Surmiak *et al.*, LTB(4) and 5-oxo-ETE from extracellular vesicles stimulate neutrophils in granulomatosis with polyangiitis. *J. Lipid Res.* **61**, 1–9 (2020).
46. S. Etienne-Manneville, A. Hall, Cdc42 regulates GSK-3beta and adenomatous polyposis coli to control cell polarity. *Nature* **421**, 753–756 (2003).
47. A. Kodama, T. Lechler, E. Fuchs, Coordinating cytoskeletal tracks to polarize cellular movements. *J. Cell Biol.* **167**, 203–207 (2004).
48. J. Liu, X. Cao, Cellular and molecular regulation of innate inflammatory responses. *Cell Mol. Immunol.* **13**, 711–721 (2016).
49. A. P. Perera *et al.*, MCC950, a specific small molecule inhibitor of NLRP3 inflammasome attenuates colonic inflammation in spontaneous colitis mice. *Sci. Rep.* **8**, 8618 (2018).
50. G. P. van Hout *et al.*, The selective NLRP3-inflammasome inhibitor MCC950 reduces infarct size and preserves cardiac function in a pig model of myocardial infarction. *Eur. Heart J.* **38**, 828–836 (2017).
51. R. Gao *et al.*, The selective NLRP3-inflammasome inhibitor MCC950 reduces myocardial fibrosis and improves cardiac remodeling in a mouse model of myocardial infarction. *Int. Immunopharmacol.* **74**, 105575 (2019).
52. O. C. Rodriguez *et al.*, Conserved microtubule-actin interactions in cell movement and morphogenesis. *Nat. Cell Biol.* **5**, 599–609 (2003).
53. T. Wittmann, C. M. Waterman-Storer, Cell motility: Can Rho GTPases and microtubules point the way? *J. Cell Sci.* **114**, 3795–3803 (2001).
54. V. Niggli, Microtubule-disruption-induced and chemotactic-peptide-induced migration of human neutrophils: Implications for differential sets of signalling pathways. *J. Cell Sci.* **116**, 813–822 (2003).